









## Sizing parabolic trough solar thermal collector networks for Industrial Application – Case study

### Dimensionamiento de redes termo solares de colectores parabólicos en aplicación Industrial – Caso de estudio

Lizárraga-Morazán, Juan-Ramón<sup>a</sup> & Picón-Núñez, Martín\*<sup>b</sup>

<sup>a</sup>  Universidad de Guanajuato •  KXB-6991-2024  0000-0002-7733-5621 •  83138

<sup>b</sup>  Universidad de Guanajuato •  AHA-5481-2022  0000-0002-0793-192X •  12408

#### SECIHTI classification:

Area: Engineering  
Field: Engineering  
Discipline: Energy engineering  
Subdiscipline: Solar energy

 <https://doi.org/10.35429/JRE.2025.9.21.3.1.11>

#### Article History:

Received: June 20, 2025

Accepted: December 10, 2025

\*  [\[picon@ugto.mx\]](mailto:picon@ugto.mx)

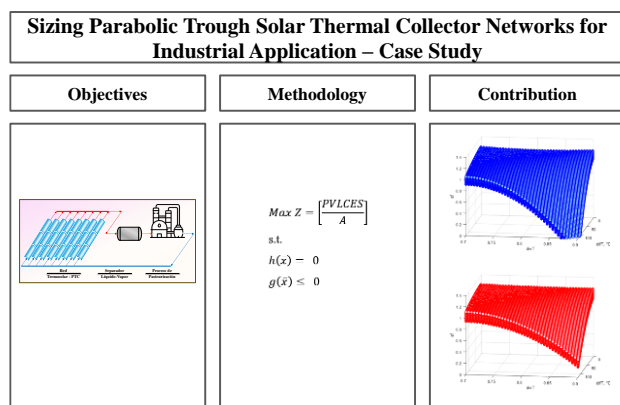


#### Abstract

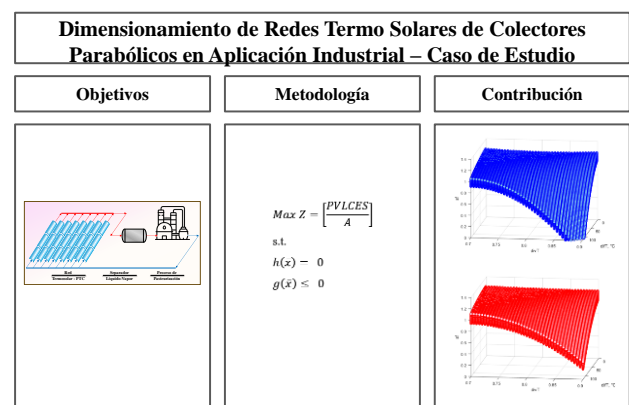
Most studies currently available in the open literature on solar thermal network designs using parabolic trough collector (PTC) technology are highly specific and complex, making them difficult to apply for initial design assessments. This work proposes a simple and broadly applicable design methodology based on previously optimised networks. It enables the determination of the required surface area as a function of inlet temperature, the thermal load and temperature required by the process, and the solar fraction. Simple polynomial correlations between design variables are identified, validated with information from operating networks reported in open literature. An example application in an existing solar thermal plant is also presented. Comparing the results with operating systems shows that the proposed model yields network areas that are 40% to 81% smaller, while achieving solar fractions in the range of 1 to 1.2.

#### Resumen

Los estudios reportados hasta ahora en la literatura abierta sobre diseños de redes termo solares que operan con tecnología de concentradores de canal parabólico (PTC) resultan específicos y complejos, lo que dificulta su aplicación para una primera aproximación. En este trabajo se propone una metodología sencilla de diseño de amplia aplicación, basada en redes previamente optimizadas para la determinación del área superficial requerida como una función de la temperatura de entrada, de la temperatura y carga térmica requeridas por el proceso y la fracción solar. Se identifican correlaciones polinómicas sencillas entre variables de diseño, validadas con información de redes en operación reportadas en literatura abierta. Además, se desarrolla un ejemplo de aplicación en una planta termo solar existente. La comparación de los resultados con sistemas existentes en operación muestra que el modelo reporta redes con áreas menores entre un 40 y 81 %, cumpliendo con fracciones solares en el intervalo de 1 a 1.2.



Solar, Fracción, Optimización, Energía, Industriales, Procesos.



Solar, fraction, optimization, Heat, Industrial, Processes

Area: Development of strategic leading-edge technologies and open innovation for social transformation

**Citation:** Lizárraga-Morazán, Juan-Ramón & Picón-Núñez, Martín. [2025]. Incorporation of Zinc Oxide Nanoparticles in Ceramic Materials. Sizing parabolic trough solar thermal collector networks for Industrial Application – Case study. Journal Renewable Energy. 9[21] 1-11: e30921111.



ISSN 2523-6881/© 2009 The Author[s]. Published by ECORFAN-Mexico, S.C. for its Holding Republic of Peru on behalf of Journal Renewable Energy. This is an open access article under the CC BY-NC-ND license [<http://creativecommons.org/licenses/by-nc-nd/4.0/>]

Peer Review under the responsibility of the Scientific Committee MARVID® - in contribution to the scientific, technological and innovation Peer Review Process by training Human Resources for the continuity in the Critical Analysis of International Research.



## Introduction

The use of clean energy is becoming increasingly urgent. Fossil fuels have harmful effects on the environment and human health, and their prices continue to rise due to the costs of extraction (Khoo & Tan, 2006) and geopolitical events—such as conflicts in the Middle East—that create uncertainty in global supply and distribution. Solar energy stands out as one of the most promising options in the transition to clean energy, with the potential to meet up to 3,500 times the total energy demand projected for humanity in the year 2050 (IEA, 2018).

The industrial sector consumes between 32% to 35% of the total energy generated worldwide (IRENA, 2024). The thermal demand of industrial processes can be met by solar thermal systems known as SHIP (Solar Heat for Industrial Processes) which include technologies such as flat plate solar collectors (FPC), evacuated tube collectors (ETC), parabolic troughs (PTC), and compound parabolic concentrators (CPC) (Ituna-Yudonago et al., 2025). Among these, the most used technology today is the PTC type, representing 90% of the installed SHIP systems worldwide (REN21, 2023). Due to its high operational flexibility, with a wide temperature range from 50 to 400 °C (Kalogirou, 2009), the PTC collector offers opportunities in industrial heating, desalination, and hybrid energy systems (Mondal & Maji, 2025).

Optimisation is a tool commonly used in the design of equipment such as solar energy collectors and solar thermal networks. Some studies have proposed improvements to the internal design of solar energy collection systems. Rabienataj et al., 2025 conducted an optimisation study to determine the best geometry for receiver tubes, enhancing thermal performance using neural networks and numerical simulations. Yin et al., 2024 analyzed various configurations of the PTC collector, considering optical, economic, and thermodynamic factors. They concluded that a width of 8.2 m and a receiver tube diameter of 90 mm are the recommended design dimensions. Shaikh & Modi, 2025 proposed a hybrid solar plant combining PTC technology and Linear Fresnel Reflectors, with two thermal storage tanks to generate electricity via a Rankine steam power cycle.

The optimisation included a thermo-economic factor through parametric analysis. It minimised the levelized cost of electricity (LCOE). Their analysis increased the plant's capacity factor by 70% and reduced the LCOE by 20% compared to a conventional plant. Zeng et al., 2025 designed a Combined Cooling, Heating, and Power (CCHP) system powered by solar energy with thermal storage, to meet the energy demand of a 1000 m<sup>2</sup> building throughout the year.

The researchers improved efficiency by optimising inlet conditions and ammonia concentration before the turbine, achieving economic savings of up to \$23,600 USD annually. Naaim et al., 2025 carried out an optimisation study in PTC systems using Monte Carlo Raytracing with a nanofluid containing 4% concentrations of Al<sub>2</sub>O<sub>3</sub>, Cu, and Ag in Therminol VP-1. Apart from increasing thermal conductivity, heat capacity, density, and viscosity, the nanoparticles improved optical performance and thermal flow distribution during operation. González-Mora & Durán-García, 2024 studied the optimal solar thermal configuration for direct steam power generation plants operating under identical conditions and geographic location.

They used PTC and Linear Fresnel Reflector (LFR) technologies. The optimisation aimed to maximise cycle efficiency. The researchers found that solar fields with 14 PTC loops performed better than those with 3 LFR loops, providing higher thermal efficiency and greater thermal storage capacity. Eskandari, 2023 designed a geothermal-solar power plant for electricity generation, heating, and cooling for the yeast industry.

The integrated system included a binary flash geothermal cycle, a PTC collector field, an auxiliary heater, a single-effect absorption chiller, and heat exchangers. Energy, exergy, and exergoeconomic analyses and parametric methods were applied. System optimisation was performed using a genetic algorithm. Under steady conditions, the energy and exergy efficiencies were 10.78% and 23.1%, respectively. The optimised exergy efficiency under ideal conditions reached 33.8%.

Other works have studied the inclusion of new systems or equipment into solar thermal networks using engineering software. [Alghorayshi et al., 2024](#) studied and analysed different renewable sources for energy production in ASPEN Plus, including biomass and solar energy, to produce power, fuel (syngas – CO and H<sub>2</sub>), and fresh water using a four-stage distillation system for seawater desalination. The solar thermal network designed with PTC technology covered an area of 38,908 m<sup>2</sup>.

The authors concluded that combining solar and biomass resources is a viable option for meeting growing demand for water, electricity, and fuel. [Contreras et al., 2023](#) developed a mathematical and numerical tool using SOLEEC software coded in MATLAB to evaluate a Direct Steam Generation (DSG) system with PTC technology in a combined power cycle. The model was based on a power plant in Mexico, showing that switching to DSG could reduce the solar field area by approximately 35%. [Arias-Velasquez et al., 2024](#) proposed a methodology to design a 150 MW plant at the Arequipa solar park in Peru.

Their design included 7,399 cylindrical cavity HE54 heliostats in a tower reactor with molten salt (MS) thermal storage. The design featured two systems: one using PTC technology, and another integrating a heliostat thermal field. Energy, exergy, and economic analysis were performed using EES software. Results showed that exergy efficiency increased by around 6% in System 1 and 2% in System 2, with annual revenue of \$34.87 million over a 20-year lifespan. [Altiokka et al., 2023](#) investigated the design of a Solar Driven Absorption Cooling System (SACS) with thermal energy storage (TES) for operation under low solar radiation, addressing cooling demand for a 120 m<sup>2</sup> residence.

The study compared four collector technologies: PTC (parabolic trough), FPC (flat plate), ETC (evacuated tube), and CPC (compound parabolic). Their thermo-economic analysis found ETC to be the most cost-effective, while PTC was the most efficient. [Cuce et al., 2024](#) conducted a study on Concentrating Solar Power (CSP) systems for cogeneration, finding that focal collectors such as Parabolic Dish Collectors (PDC) can reach higher process temperatures.

However, they are more expensive and require larger installation areas compared to linear-focus systems like PTC, which can reach temperatures up to 800 °C. [Kessentini et al., 2023](#) described, developed, and operated a hybrid mini power plant with direct steam generation (DSG) using PTC technology in the southern Mediterranean region under the REECOOP (Renewable Electricity Cooperation) project. The plant was designed and tested under daily conditions, yielding valuable operational and control data for both conventional and hybrid modes. [Zhao et al., 2024](#) studied two PTC systems: one ideal system using multiple concentration ratios (CR) across different sections, and a multi-section system applying practical CRs. They developed a two-dimensional thermal prediction model using the finite volume method. In the operating range of 293°C to 393 °C, the multi-section system achieved 6.7% higher optical efficiency and a 4.5% increase in thermal efficiency compared to the conventional system.

From the literature review, it is evident that the sizing of solar thermal plants using PTC technology for different applications remains an underexplored topic as in most applications, it is not established whether the designs are viable or if they meet the specific requirements of the processes. On the other hand, existing design methodologies tend to be complex, which limits their practical applicability in industrial settings that demand precise yet easily implementable solutions.

This study aims to present a simple and validated design methodology based on previously optimised network structures. The proposed approach enables the effective determination of the collector area, inlet temperature, and solar fraction of a PTC solar thermal network applied to industrial processes (SHIP), using only the process's target temperature and thermal load requirements as input parameters. Finally, a practical example is included to demonstrate the application of the proposed methodology.

## Methodology

The methodology for obtaining operational and design data for optimised solar thermal networks in industrial processes is based on the work published by [Lizárraga-Morazan & Picón-Núñez, 2024a](#).

A Particle Swarm Optimization (PSO) problem was solved using a transient thermo-hydraulic-economic model, validated under typical daily conditions in winter and summer, to determine the size (area) and structure (PTC geometry that defines the network) needed to meet a thermal load, given a mass flow rate and the type of heat transfer fluid (HTF). Sampling was carried out by varying the thermal load  $Q_p$ , the process's target temperature  $T_{obj}$ , and the inlet temperature  $T_{in}$  to generate a set of optimized points. The target temperature was set at seven values: 70°C, 125°C, 180°C, 235°C, 293°C, 345°C, and 400°C; the thermal load values chosen were: 400 kW, 1,600 kW, 2,800 kW, and 4,000 kW; and the different values of inlet temperature were related to the objective temperature as follows: 0.7, 0.8, and  $0.9 \cdot T_{obj}$ . Instantaneous daily environmental data were collected in the city of Guanajuato (21.0190° N, 101.2574° W). The optimisation problem was solved for each of the 84 variable combinations and for the typical days representing winter and summer seasons.

The solar fraction for each optimised point in both seasonal samples was obtained using the following expression:

$$sf = \frac{Q}{Q_p} \quad [1]$$

Where  $sf$  is the solar fraction,  $Q$  represents the useful thermal load generated by the optimised network during its operation, and  $Q_p$  is the thermal load required by the process. The mean optimised  $sf$  values for the winter and summer seasons, respectively are  $1.05 \pm 0.09$  and  $1.06 \pm 0.08$ , with minimum and maximum values of 0.81 and 1.2, and 0.9 and 1.23 (Lizárraga-Morazán & Picón-Núñez, 2024b). To develop correlations based on these results that allow network design as a function of process variables, the solar fraction  $sf$  and the network area  $A$  were defined as independent variables. Additionally, the following independent variables were established:  $d_{if}T = T_{obj} - T_{in}$ ;  $d_{iv}T = \frac{T_{in}}{T_{obj}}$ ; and  $Q_p$ . Various fitting expressions were evaluated, with the best correlations obtained using polynomial equations. The relationships between the independent variables and the corresponding design variables from the highest-fitting correlations are presented below:

$$\begin{aligned} sf &= sf(d_{if}T, d_{iv}T, Q_p) \\ A &= A(sf, Q_p) \end{aligned} \quad [2]$$

The validity of the resulting correlations was verified by comparing them to the areas of existing solar thermal networks. Finally, a representative case study was selected to demonstrate the practical application of the calculation methodology.

## Results

The expression used to determine the solar fraction is as follows:

$$\begin{aligned} sf &= sf(x_1, x_2, x_3) = w_1 + w_2x_1^2 + \\ &w_3x_1 + w_4x_2^2 + w_5x_2 + w_6x_1x_2 + \\ &w_7x_1x_2^2 + w_8x_2x_1^2 + w_9x_3 + w_{10}x_1x_3^2 + \\ &w_{11}x_2x_3^2 + w_{12}x_3x_1^2 \end{aligned} \quad [3]$$

Where  $x_1 = d_{if}T$ ,  $x_2 = d_{iv}T$ ,  $x_3 = Q_p$ . The correlation used to calculate the area of the solar thermal network is presented below:

$$\begin{aligned} A &= A(x_1, x_2) = w_1 + w_2x_1^2 + w_3x_1 + \\ &w_4x_2^2 + w_5x_2 + w_6x_1x_2 + w_7x_1x_2^2 + \\ &w_8x_2x_1^2 \end{aligned} \quad [4]$$

Where  $x_1 = sf$ ,  $x_2 = Q_p$

Tables 1 and 2 show the values of the correlation constants (weights) for equations [3] and [4], respectively.

## Box 1

**Table 1**

Correlation [3] weights

$w_i$	Winter	Summer
1	4.381659035	2.702525781
2	0.0002618105	0.0001238720
3	-0.184758884	-0.101122509
4	4.94884E+00	2.18736E+00
5	-7.909089401	-3.545451963
6	0.4732791705	0.2639712102
7	-0.300857338	-0.171581734
8	-3.81988E-04	-1.85823E-04
9	-7.65424E-05	-0.000112347
10	3.887883E-11	2.876322E-11
11	8.312521E-09	1.605053E-08
12	-5.74657E-10	0.000000000

Source: Own elaboration.

**Box 2**

**Table 2**

Correlation [4] weights

$w_i$	Winter	Summer
1	1698.522158	7725.614716
2	-940.0668403	5238.198464
3	-427.0328683	-12692.56241
4	8.642521E-04	2.746293E-04
5	0.185405954	-1.638407765
6	-0.922892605	4.5701634793
7	-0.000816573	-0.000277020
8	2.405315536	-1.467934015

Source: Own elaboration.

Table 3 summarizes the results of a statistical analysis for the correlations obtained for both the solar fraction and the area, across both seasons.

**Box 3**

**Table 3**

Multivariate polynomial regression statistics

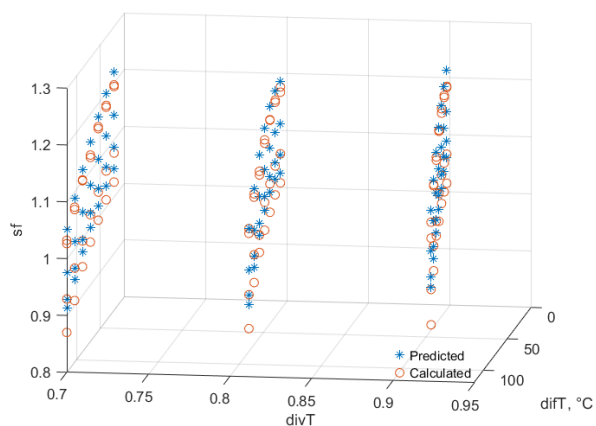
	Winter		Summer	
	$sf$	$A$	$sf$	$A$
MSE	1.9e-4	149.3	9.0e-5	67.3
RMSE	4.3e-2	12.2	9.5e-3	8.2
$R^2$	0.98	1.00	0.99	1.00
$R^2_{adj}$	0.97	1.00	0.99	1.00

Source: Own elaboration.

Figure 1 displays the graphical fit of the polynomial regression for the solar fraction during winter and summer.

**Box 4**

(a)



(b)

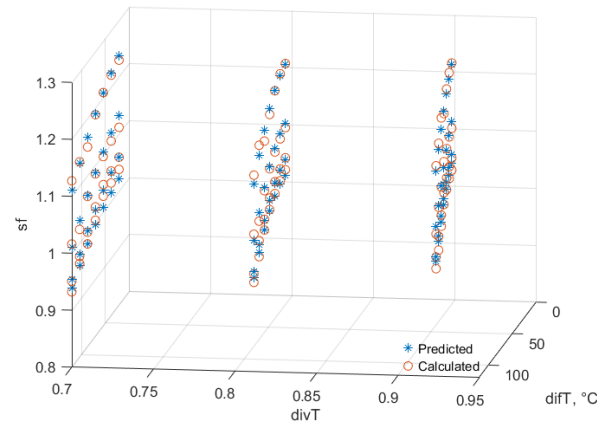


**Figure 1**

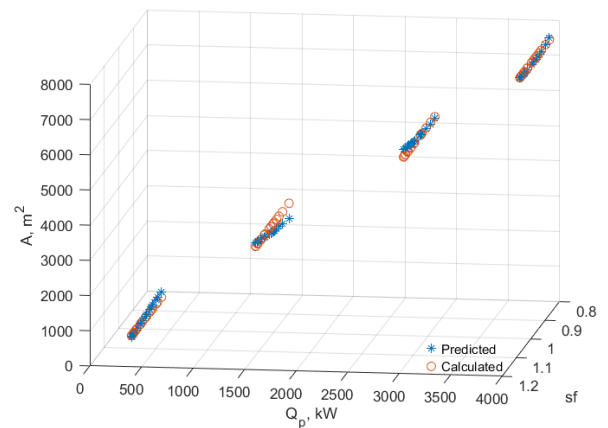
Fitness of the  $sf$ - $A$  regression model: (a) winter and (b) summer.

Source: Own elaboration

Figure 2 presents the fit of the correlation used to determine the network area.

**Box 5**

(a)



(b)

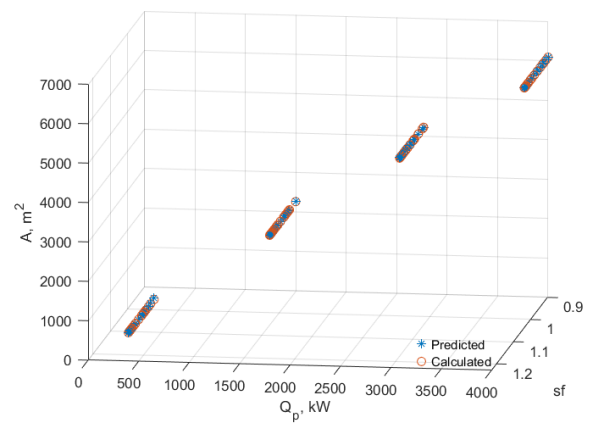


**Figure 2**

$sf$  -  $A$  performance profile: (a) winter, and (b) summer.

Source: Own elaboration

Figure 3 illustrates the behavior of the solar fraction with respect to the independent variables  $d_{if}T$  and  $D_{iv}T$ .

### Box 6

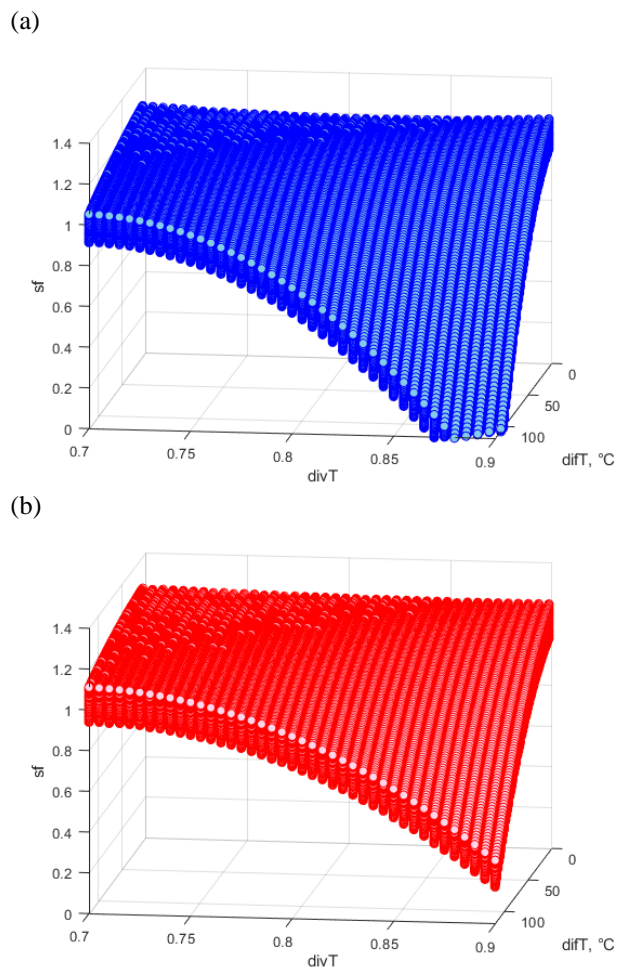


**Figure 3**  
 $sf - d_{iv}T - d_{if}T$  performance profile: (a) winter, and (b) summer.

Source: Own Elaboration

Figure 4 illustrates the behavior of the solar fraction with respect to the thermal load  $Q_p$  and the temperature gradient  $d_{if}T$ .

### Box 7

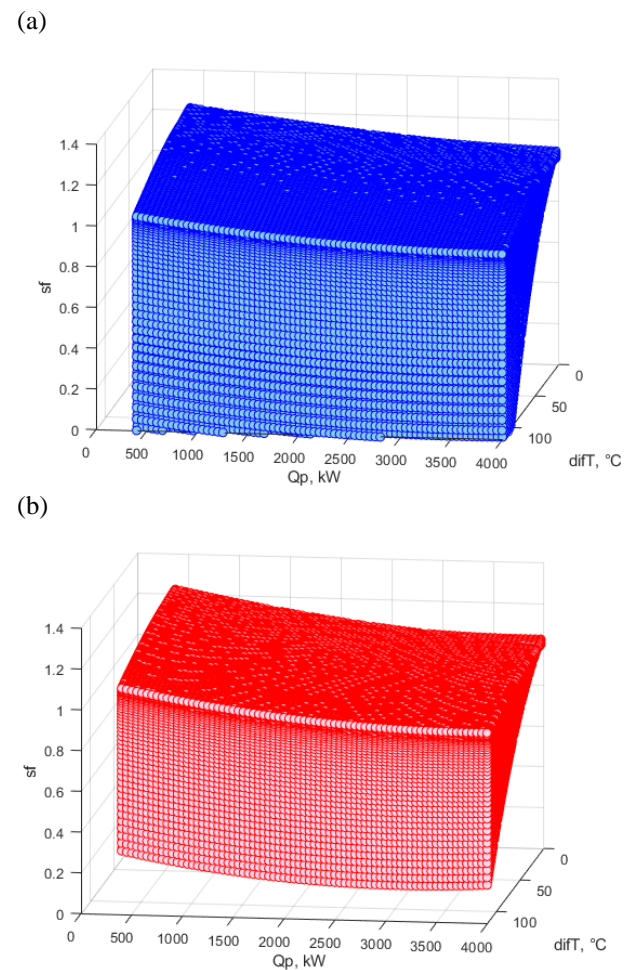
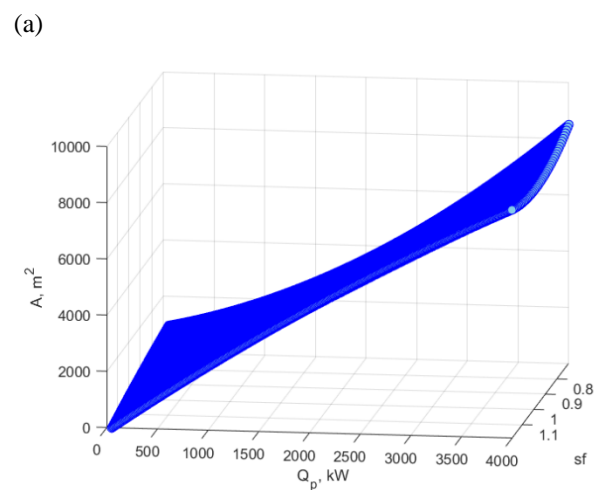


**Figure 4**  
 $sf - Q_p - d_{if}T$  performance profile: (a) winter, and (b) summer.

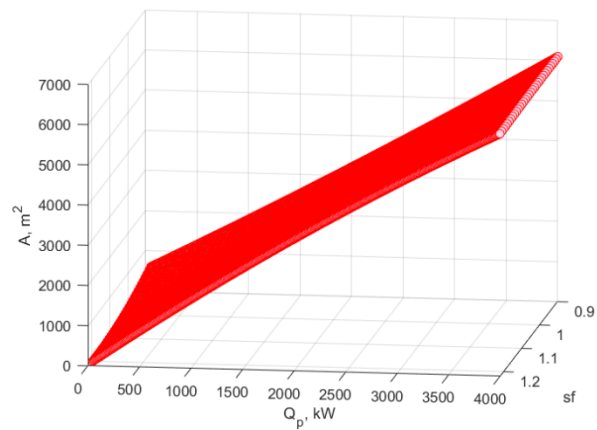
Source: Own Elaboration

Figure 5 shows the profile of the network area as a function of the thermal load and the solar fraction.

### Box 8



(b)

**Figure 5**

$A - Q_p - sf$  performance profile: (a) winter, and (b) summer.

Source: Own elaboration

The validation of the thermo-hydraulic model used to solve the network optimization problem was reported in the work by Lizárraga-Morazán & Picón-Núñez, 2024a. Table 4 presents a comparison between the installed area (A) and the average area ( $A_{calc}$ ) obtained using correlations [3] and [4], for several solar thermal networks reported in the literature. The thermal load values fall within the range covered by the correlations. The networks referred to as Sello Rojo Lechera and Centro Cooperativo los Altos were reported by Rodríguez Rodrigo et al., 2024; Frito Lay by Schoeneberger et al., 2020; and Phoenix Correctional Institution by May et al., 2000. In these comparisons, the area calculated using the correlations was lower than the installed area, by a range of 46% to 81%.

### Box 9

**Table 4**

SHIP's installed area comparison

Entity	Location	A, m <sup>2</sup>	Q kW	$A_{ca}$ , m <sup>2</sup>	%
Frito Lay	Modesto, California, USA	5,017	492	965	81
Sello Rojo Lechera	Guadalajara, Jal, Mx	1,641	240	429	74
Centro Lechero Cooperativo Los Altos	Arandas, Jal, Mx	422	94.5	136	68
Phoenix Federal Correctional Institution	Arizona, USA	1,584	440	858	46

Source: Own elaboration.

Table 5 presents a comparison of the installed area of industrial solar thermal networks using PTC technology currently in operation in Mexico (Ituna-Yudonago et al., 2025), against the area calculated using the proposed correlations. In this case, the calculated areas were lower by a range of 60% to 68%.

### Box 10

**Table 5**

Mexican SHIP's installed area comparison

Sector	Reported	Acalc	%
Food	A [m <sup>2</sup> ]	1,067	68
	3,366.83		
	60-120 °C		
	Q [kW]		
	541.51		
Dairy	A [m <sup>2</sup> ]	2,000	63
	5,508.40		
	60-120 °C		
	Q [kW]		
	1,010.60		
Agro-Industry	A [m <sup>2</sup> ]	1,503	60
	3,725.38		
	60-120 °C		
	Q [kW]		
	757.91		
Beverage	A [m <sup>2</sup> ]	685	66
	2,003.88		
	60-90 °C		
	Q [kW]		
	354.94		

Source: Own elaboration.

### Case Study

The following section describes the design procedure of an industrial solar thermal plant. For comparison purposes, the data used is from a plant currently in operation. The network supplies hot water at a temperature of 78 °C to a milk pasteurization plant located in Guadalajara, Jalisco, Mexico (Figure 6). The installed area is 1,641 m<sup>2</sup>, with a thermal load generation of 360.88 kW. The outlet temperature of the thermal fluid is 68 °C. The objective is to determine the optimised area of the solar thermal network and analyse the effect of varying the inlet temperature.

## Box 11

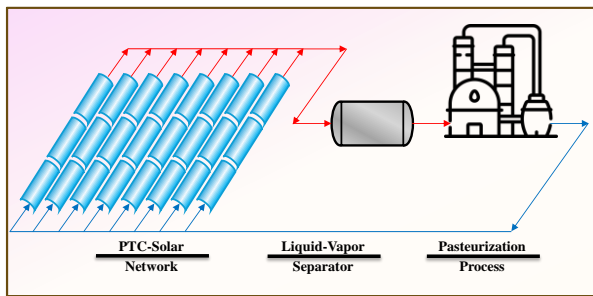


Figure 6

Plant Layout for case study.

Source: Own elaboration

The design data are summarised in Table 6.

## Box 12

Table 6

Case Study data

Data	Value
$T_{obj}$ , [°C]	78
$T_{in}$ , [°C]	58
$Q_p$ , [kW]	360.88
$A$ , [m <sup>2</sup> ]	1,641

Source: Own Elaboration.

The temperature variables are  $difT = 20$  °C and  $divT = 0.743$ . Using Equation [3], the solar fraction is determined for summer and winter seasons, resulting in 1.24 and 1.22, respectively. The network area is calculated using Equation [4], resulting in 669.6 m<sup>2</sup> and 716.3 m<sup>2</sup>. The optimised areas for winter and summer are 59.2% and 72.8% lower than the reported value, respectively. A design area must be defined based on these results. Accordingly, the winter value (716.3 m<sup>2</sup>) is selected as the design area. A parametric analysis was conducted by varying the inlet temperature to determine its impact on the solar fraction and network area. The results are shown in Table 7.

## Box 13

Table 7

Parametric analysis

$T_{in}$	Summer		Winter		$A_{summer} - A_{winter}$
[°C]	$sf$	$A$ [m <sup>2</sup> ]	$sf$	$A$ [m <sup>2</sup> ]	[m <sup>2</sup> ]
68	1.22	660.4	1.21	728.4	68.0
58	1.24	669.6	1.22	716.3	46.8
48	1.21	657.4	1.16	773.5	116.2
38	0.99	837.0	0.77	1,164.9	328.0
33	0.74	1,544	0.37	1,544.0	0

Source: Own elaboration.

From Table 7, an inlet temperature of  $T_{in} = 58$  °C yields the maximum solar fraction for both seasons (1.24 for summer and 1.22 for winter). Figure 7 graphically represents the impact of  $T_{in}$  on both the network area and solar fraction in each season. Within the inlet temperature range of 50°C to 70 °C, the area and solar fraction remain relatively constant (see Figure 7).

The parametric analysis indicates that an inlet temperature of 58 °C is the most suitable, as it results in the highest solar fractions for both seasons and produces small and comparable design areas.

## Box 14

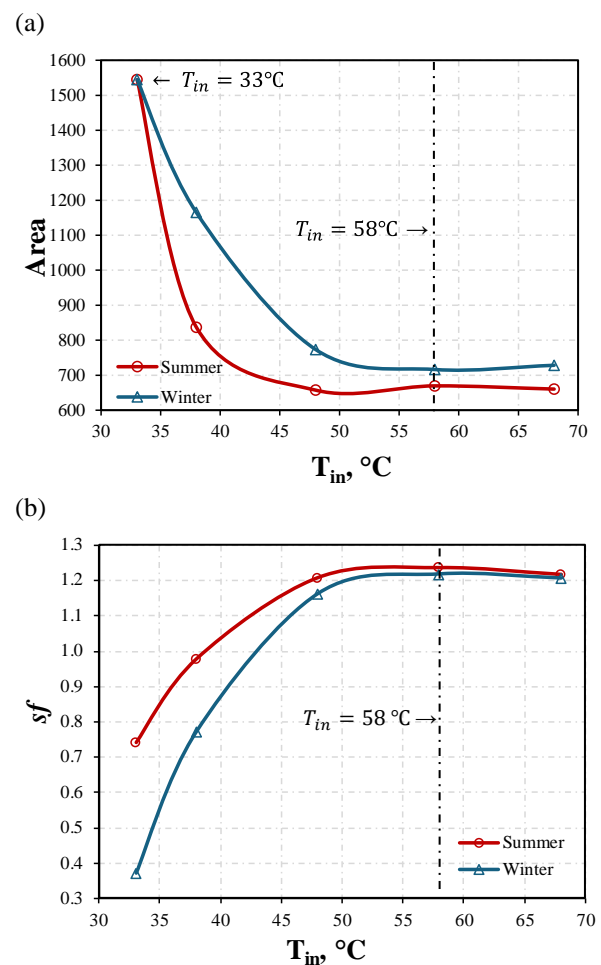


Figure 7.

Effect of  $T_{in}$  on (a)  $sf$  (b)  $A$ .

Source: Own elaboration

## Conclusions

Based on the results of this work, the following conclusions are drawn:

1. The proposed expressions allow for the design of optimised SHIP plants based on three key variables: inlet temperature, objective process temperature, and required thermal load.
2. The solar thermal networks designed exhibit high flexibility, capable of maintaining elevated solar fractions across a wide range of inlet temperatures without modifying the collector area.
3. It is noteworthy that the network designs obtained are between 40% and 81% smaller compared to reported values, while maintaining superior solar fractions in the range of 1.1 to 1.2.
4. Inlet temperature and thermal load directly affect the required area and solar fraction: lower inlet temperatures or higher thermal loads lead to greater area requirements.
5. The polynomial regression models used enable effective prediction of the behavior of solar fraction and network area variables across different seasons.

## Declarations

## Conflict of interest

The authors declare no interest conflict. They have no known competing financial interests or personal relationships that could have appeared to influence the article reported in this article.

## Authors' Contribution

*Juan-Ramón Lizárraga-Morazán*: Contributed to the research methodology and generation of results and writing of the manuscript.

*Martín Picón-Núñez*: Contributed to the project idea, research method, editing and revising of the manuscript.

## Funding

No funding was received for the development of this research.

## Acknowledgements

CONAHCYT is greatly acknowledged for the postdoctoral grant awarded to Dr. Juan-Ramón Lizárraga-Morazán.

## Abbreviations

<i>HTF</i>	Heat transfer fluid
<i>SHIP</i>	Solar heat for industrial processes

## Nomenclature

$A$	Network area, [m <sup>2</sup> ]
$Q$	Useful heat, [kW]
$Q_p$	Process heat, [kW]
$sf$	Solar fraction
$T_{in}$	HTF Inlet temperature, [°C]
$T_{obj}$	HTF target temperature, [°C]

## References

### Basics

IEA. (2018). *Clean and efficient heat for industry*. IEA, Paris. Accessed: Jul. 11, 2025. [Online]. Available: <https://www.iea.org/commentaries/clean-and-efficient-heat-for-industry>

IRENA. (2024). *RENEWABLE CAPACITY STATISTICS 2024*. [Online]. Available: [https://www.irena.org/-/media/Files/IRENA/Agency/Publication/2024/Mar/IRENA\\_RE\\_Capacity\\_Statistics\\_2024.pdf](https://www.irena.org/-/media/Files/IRENA/Agency/Publication/2024/Mar/IRENA_RE_Capacity_Statistics_2024.pdf)

### Differences

Alghorayshi, S. T. K., Imandoust, M., Hemmatzadeh, A., Abbasi, S., Javidfar, M., Seifollahi, M., Gitifar, S., & Zahedi, R. (2024). Design, simulation and investigation of the tri-generation process of fresh water, power and biogas using solar thermal energy and sewage sludge. *Chemical Engineering Research and Design*, 208, 242–257. doi:10.1016/J.CHERD.2024.07.009

Arias-Velasquez, R. M. (2024). Methodology for the Design Solar Thermal Station: Case Study of 150 MW for Arequipa. *2024 IEEE ANDESCON*, 1–6. doi:10.1109/ANDESCON61840.2024.10755776

Altioikka, G., Banu, A., Oğuz, A. (2023). Design and optimization of absorption cooling system operating under low solar radiation for residential use. *Journal of Building Engineering*, 73. <https://doi.org/10.1016/J.JOBE.2023.106697>

- Cuce, P. M., Guclu, T., & Cuce, E. (2024). Design, modelling, environmental, economic and performance analysis of parabolic trough solar collector (PTC) based cogeneration systems assisted by thermoelectric generators (TEGs). *Sustainable Energy Technologies and Assessments*, 64, 103745. doi: 10.1016/J.SETA.2024.103745
- Contreras, E., Saldaña, J. G. B., Alejo, J. de la C., Torres, C. D. C. G., Bernal, J. A. J., & Vazquez, M. B. A. (2023). A Feasibility Analysis of a Solar Power Plant with Direct Steam Generation System in Sonora, Mexico. *Energies*, 16(11). doi: 10.3390/en16114388
- Eskandari, A. (2023). Design, 3E scrutiny, and multi-criteria optimization of a trigeneration plant centered on geothermal and solar energy, using PTC and flash binary cycle. *Sustainable Energy Technologies and Assessments*, 55, 102718. doi: 10.1016/J.SETA.2022.102718
- González-Mora, E., & Durán-García, M. D. (2024). Assessing parabolic trough collectors and linear Fresnel reflectors direct steam generation solar power plants in Northwest México. *Renewable Energy*, 228, 120375. doi:10.1016/J.RENENE.2024.120375
- Ituna-Yudonago, J. F., García-Valladares, O., Ortiz-Rodríguez, N. M., Ibarra-Bahena, J., & Galindo-Luna, Y. R. (2025). Applications of solar thermal technologies in Mexican industries for heating processes and their contribution against global warming: An overview. *Solar Energy*, 291, 113395. doi:10.1016/J.SOLENER.2025.113395
- Kalogirou, S. (2009). *Solar energy engineering: Process and systems*. London UK, 49–89.
- Kessentini, H., Ferchichi, S., & Bouden, C. (2023). Design, commissioning and operation of a mini hybrid parabolic trough solar thermal power plant for direct steam generation. *Solar Energy Advances*, 3, 100039. doi:10.1016/J.SEJA.2023.100039
- Khoo, H. H., & Tan, R. B. H. (2006). Environmental Impact Evaluation of Conventional Fossil Fuel Production (Oil and Natural Gas) and Enhanced Resource Recovery with Potential CO<sub>2</sub> Sequestration. *Energy & Fuels*, 20(5), 1914–1924. doi:10.1021/ef060075+
- Lizárraga-Morazan, J. R., & Picón-Núñez, M. (2024a). Harnessing solar power in industry: Heuristic optimisation design and transient thermal modelling of parabolic trough solar collector networks. *Chemical Engineering and Processing - Process Intensification*, 200, 109776. doi:10.1016/J.CEP.2024.109776
- Lizárraga-Morazán, J. R., & Picón-Núñez, M. (2024b). Determination of the solar fraction for optimized parabolic concentrator solar collector networks. *ECORFAN-Journal Democratic Republic of Congo*, 10(18), 1–9. doi:10.35429/EJDRC.2024.10.18.1.9
- Mondal, B., & Maji, A. (2025). A brief review on analysis and recent development of parabolic trough collector. *Energy Storage and Saving*, 4(2), 123–132. doi:10.1016/J.ENSS.2024.12.003
- Naaim, S., Ouhammou, B., El Merabet, Y., Aggour, M., Mihi, M., el Mers, E. M., & Daouchi, B. (2025). Optimization of Nanoparticle Concentration for Enhanced Performance of Therminol® VP-1-Based Nanofluids in Parabolic Trough Systems. *Results in Engineering*, 26, 105051. doi:10.1016/j.rineng.2025.105051
- Rabienataj Darzi, A. A., Razbin, M., Allahdadi, A., Mousavi, S. M., Taylor, R. A., & Li, M. (2025). Designing high-efficiency parabolic trough receiver tubes via AI-assisted simulation. *Renewable Energy*, 251, 123366. doi:10.1016/J.RENENE.2025.123366
- REN21. (2023). *RENEWABLES 2023 GLOBAL STATUS REPORT*. Renewables Now. [Online]. Available: [https://www.ren21.net/wp-content/uploads/2019/05/GSR2023\\_GlobalOverview\\_Full\\_Report\\_with\\_endnotes\\_web.pdf](https://www.ren21.net/wp-content/uploads/2019/05/GSR2023_GlobalOverview_Full_Report_with_endnotes_web.pdf)
- Shaikh, I., & Modi, A. (2025). A novel concentrating solar plant configuration with multiple solar fields and thermal energy storage to reduce energy production costs. *Case Studies in Thermal Engineering*, 71, 106185. doi:10.1016/J.CSITE.2025.106185
- Yin, H., Sun, Y., Zhang, J., Che, S., Zhang, X., & Xing, Y. (2024). Engineering optics and thermodynamics design of parabolic trough solar collector. *Journal of Physics: Conference Series*, 2782, 12038. doi:10.1088/1742-6596/2782/1/012038

Zeng, J., Yin, S., Tong, L., Liu, C., Wang, L., & Wu, C. Y. (2025). [Design and evaluation of an integrated CCHP system based on solar thermal supplementary heating and off-peak electrical thermal storage heating](#). *Energy*, 328, 136505. doi: 10.1016/J.ENERGY.2025.136505

Zhao, K., Wang, X., Gai, Z., Qin, Y., Li, Y., & Jin, H. (2024). [Enhancing the efficiency of solar parabolic trough collector systems via cascaded multiple concentration ratios](#). *Journal of Cleaner Production*, 437, 140665. doi: 10.1016/J.JCLEPRO.2024.140665

## Discussions

Rodríguez Rodrigo, R., Díaz Martín, R., Baranda Fernández, M., Román Gallego, J. Á., & Mayo del Río, C. (2024). [Technical and economic study of solar energy concentration technologies \(linear Fresnel and parabolic trough collectors\) to generate process heat at medium temperature for the dairy industry of Spain](#). *Solar Energy*, 271, 112420. doi:10.1016/J.SOLENER.2024.112420

Schoeneberger, C. A., McMillan, C. A., Kurup, P., Akar, S., Margolis, R., & Masanet, E. (2020). [Solar for industrial process heat: A review of technologies, analysis approaches, and potential applications in the United States](#). *Energy*, 206, 118083. doi:10.1016/J.ENERGY.2020.118083

May, K., Barker, G., Hancock, E., Walker, A., Dominick, J., & Westby, B. (2000). [Performance of a Large Parabolic Trough Solar Water Heating System at Phoenix Federal Correctional Institution](#). *Journal of Solar Energy Engineering*, 122(4), 165–169. doi:10.1115/1.1331288